Article

Meldrum-Based-1*H*-1,2,3-Triazoles as Antidiabetic Agents: Synthesis, *In Vitro* α-Glucosidase Inhibition Activity, Molecular Docking Studies, and *In Silico* Approach

Satya Kumar Avula, Saeed Ullah, Sobia Ahsan Halim, Ajmal Khan,* Muhammad U. Anwar, René Csuk, Ahmed Al-Harrasi,* and Ali Rostami*

Read Online

ACCESS | Metrics & More | Article Recommendations | Supporting Information

ABSTRACT: A series of novel alkyl derivatives (**2**−**5a,b**) and 1*H*-1,2,3-triazole analogues (**7a**−**k**) of Meldrum's acid were synthesized in a highly effective way by using *"click"* chemistry and screened for in vitro α-glucosidase inhibitory activity to examine their antidiabetic potential. ^{1}H NMR, ^{13}C-NMR, and high-resolution electrospray ionization mass spectra (HR-ESI-MS) were used to analyze each of the newly synthesized compounds. Interestingly, these compounds demonstrated high to moderate α-glucosidase inhibitory potency having an IC$_{50}$ range of 4.63−80.21 μM. Among these derivatives, compound **7i** showed extraordinary inhibitory activity and was discovered to be several times more potent than the parent compound Meldrum (**1**) and the standard drug acarbose. Later, molecular docking was performed to understand the binding mode and the binding strength of all the compounds with the target enzyme, which revealed that all compounds are well fitted in the active site of α-glucosidase. To further ascertain the structure of compounds, suitable X-ray single crystals of compounds **5a**, **7a**, and **7h** were developed and studied. The current investigation has shown that combining 1*H*-1,2,3-triazole with the Meldrum moiety is beneficial. Furthermore, this is the first time that the aforementioned activity of these compounds has been reported.
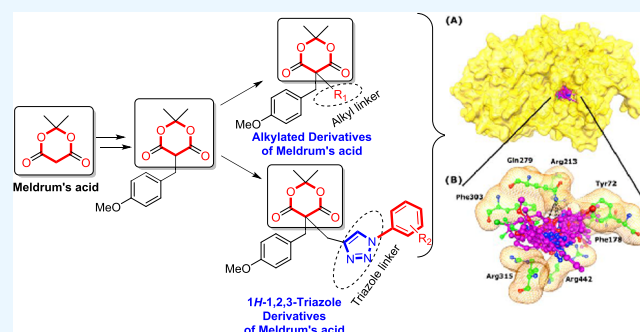
1. INTRODUCTION

Diabetes mellitus (DM) is a chronic metabolic disease and one of the leading causes of death worldwide due to its severe complications. Long-term high blood glucose levels in diabetic individuals cause several problems, including microvascular issues or the loss of extremely small blood vessels in the body, which can lead to catastrophic kidney, eye, nerve, and heart ailments.[1,2] Type 2 DM (T2DM) affects the majority of patients, and the disease prevalence is becoming a growing public health concern. The World Health Organization (WHO) predicted in 2006 that the number of patients with T2DM will rise to 366 million by 2030, accounting for 9.9% of the world's adult population. Several lifestyle variables are involved in increasing the risk of T2DM, including obesity and weight, physical inactivity, cigarette smoking, low-fiber diet with a high glycemic index, and depression.[3,4] Currently, the most effective antidiabetic therapeutic strategy is reducing blood glucose levels. Because α-glucosidase is a critical enzyme in the conversion of complex carbohydrates (polysaccharides) to simple sugars (monosaccharides), α-glucosidase inhibitors (α-GIs) have taken a unique place in drug development. α-Glucosidase is located in the brush border of the small intestine and selectively hydrolyzes terminal 1-4-α-glucosidase residues (starch or disaccharides) to produce glucose. By delaying the digestion of carbohydrates, α-GI limits the rate of glucose absorption and avoids the progression of the impaired glucose tolerance factor (GTF) to T2DM. It has been discovered that limiting the effect of dietary carbohydrates on blood sugar is critical.[5,6]

Meldrum's acid, that is, 2,2-dimethyl-1,3-dioxan-4,6-dione (R^1 = Me, R^2, R^3 = H), was prepared in 1908 by Andrew Norman Meldrum; however, the exact structure was revealed in 1948 by Davidson and Benhard (Scheme 1).[7] Meldrum's acid derivatives are bench-stable, easily accessible compounds that act as crucial organic building blocks, which are fundamental components in organic synthesis and flourishing applications in the synthesis of natural products and multi-component reactions (MCRs).[8−14] Meldrum's acid derivatives have been used as substrates for a wide range of reactions with applications in the total synthesis of natural products and the
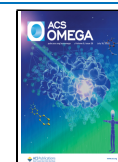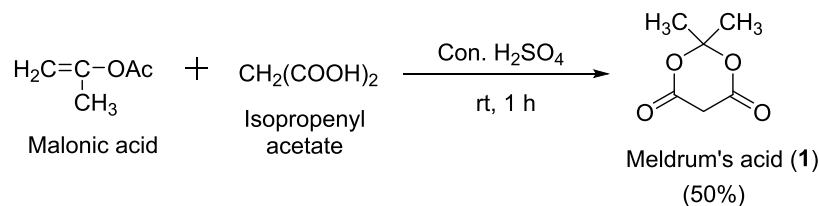
Scheme 1. Synthesis of Meldrum's Acid (1)

Malonic acid   Isopropenyl acetate   Con. H$_2$SO$_4$ / rt, 1 h   Meldrum's acid (1) (50%)

synthesis of biologically significant compounds (e.g., taiwana-quinol B),[15] at-turmerone and α-curcumene,[16] and coumarin derivatives.[17] Furthermore, this medicine is reasonably priced. Meldrum's acid (1) is regarded as a "standard" antibiotic due to its excellent antibacterial effectiveness, biological activity, and few side effects (Figure 1).[18]
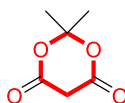

Figure 1. Chemical structure of Meldrum's acid (1).

Apart from the extensive utility in organic synthesis, Meldrum's acid derivatives show biological potential as antioxidant and antimalarial agents, including α-glucosidase and cholinesterase inhibitory activities.[19,20]

On the other hand, the use of 1H-1,2,3-triazole compounds in pharmaceuticals and agrochemicals has grown.[21] Due to its numerous and varied uses in the fields of biomedical, biochemical, and materials sciences,[22] these 1H-1,2,3-triazole compounds play a crucial role in organic chemistry. Over the last few decades, the number of compounds with a triazole moiety has significantly increased. In addition, heterocycles with 1H-1,2,3-triazole scaffolds are known to possess biological properties such as antimicrobial,[23] antibacterial,[24] antiviral,[25] anti-HIV,[26] anti-inflammatory,[27] and anticancer properties.[28] Our research group has reported several synthesized bioactive 1H-1,2,3-triazole analogues with potential biological activities including α-glucosidase inhibitors (Figure 2).[29−31]

In this context, our recommendation was to alter Meldrum's acid by adding an alkyl or N-heterocyclic moieties. To know the dual potential of these molecules, we synthesized novel derivatives of meldrum (1) linked with 1H-1,2,3-triazole, which were further tested against the α-glucosidase enzyme, and their mode of binding with the enzyme was determined through molecular docking. To the best of our knowledge, this is the first study on hybrid 1H-1,2,3-triazole derivatives with Meldrum molecules.

2. RESULTS AND DISCUSSION

2.1. Chemistry. *2.1.1. Synthesis of Alkyl Derivatives of Meldrum's Acid (2−5a,b).* The synthetic scheme of alkyl derivatives of Meldrum's acid is depicted in Scheme 2. In pursuing our aim to synthesize alkyl derivatives, we have designed and synthesized novel analogues of Meldrum. The desired alkyl derivatives of Meldrum (2−5a,b) were achieved by a three-step protocol with condensation and reduction, followed by an alkylation reaction. Thereby, in the initial step, Meldrum 1 reacted with p-anisaldehyde in pyridine at room temperature for 15 h to afford a high yield (97%) of compound 2. The following step is compound 2 undergoing reduction with NaBH$_4$ in EtOH at 0 °C to rt for 2−3 h to furnish

compound 3 in high yield (98%). The final step produced high yields (96−98%) of alkyl derivatives of Meldrum's acid (5a,b) from compound 3 when it was treated with alkyl bromide (4a,b) in a DMF solvent with potassium carbonate as a base for 18 h at room temperature (Table 1).[13,32,33]

The distinctive signals for acetylenic (−CH≡C) and propargyl methylene (−CH$_2$) protons can be seen in the ^{1}H NMR spectra of compound 5a at δ 2.09 and 2.92, respectively. Acetylene (−CH≡C−) and propargyl methylene (−CH$_2$) groups are represented by signals in the ^{13}C NMR spectra of compound 5a at δ 78.3, 72.9, and 30.2. The protonated molecular ion at (m/z) 303.2076 [M + H$^+$] was detected by HRMS (ESI), providing additional evidence of compound 5a.

Figure 3 shows the structure of compound 5a, which X-ray crystallography unambiguously confirmed. Its crystals were grown from EtOAc and dichloromethane (DCM) (1:1) solution.

2.3. Synthesis of 1H-1,2,3-Triazole Derivatives of Meldrum's Acid (7a−k). Scheme 3 illustrates the process for synthesizing Meldrum's acid 1H-1,2,3-triazole derivatives. Chemistry used in the "click" reaction produced the necessary 1H-1,2,3-triazole derivatives of Meldrum's acid (7a−k). The intended products, 1H-1,2,3-triazole derivatives of Meldrum's acid (7a−k), were produced in step 1 with high yields (96−98%) (Table 2) by reacting 5a with various substituted aromatic azides (6a−k) in the presence of Hünig's base and copper iodide (CuI) in acetonitrile (MeCN).[34−37]

By the appearance of a distinctive singlet at δ 7.50−7.93 in their respective ^{1}H NMR spectra, which can be attributed to the H-5′ proton of the triazole ring, the production of 1H-1,2,3-triazole derivatives of Meldrum's acid (7a−k) was confirmed. Furthermore, the synthesized 1H-1,2,3-triazole hybrids of Meldrum's acid (7a−k) displayed the characteristic triazole ring carbon signals between δ 120−125 and 142−145 as well as the phenyl ring carbon signals at δ 100−165 in their ^{13}C NMR spectra. HRMS provided additional support for the 1H-1,2,3-triazole Meldrum derivatives (7a−k) in terms of their structural details.

Figure 4 shows the structures of compounds 7a and 7h, which X-ray crystallography clearly validated. These two compound crystals were grown from the gradual solvent evaporation of EtOAc.

By using spectrum data analysis (^{1}H & ^{13}C NMR, HRMS, and ^{19}F NMR spectroscopy when appropriate), the structures of all the synthesized compounds (2−5a,b and 7a−k) were confirmed.

3. BIOLOGICAL ACTIVITY

The general structural feature of the synthesized Meldrum's acid derivatives (5a,b and 7a−k) are presented in Figure 5. The three changeable moieties (meldrum, alkyl, and triazole) were thought to form a stiff motif with an aromatic group connected to Meldrum's acid moiety, which primarily governs
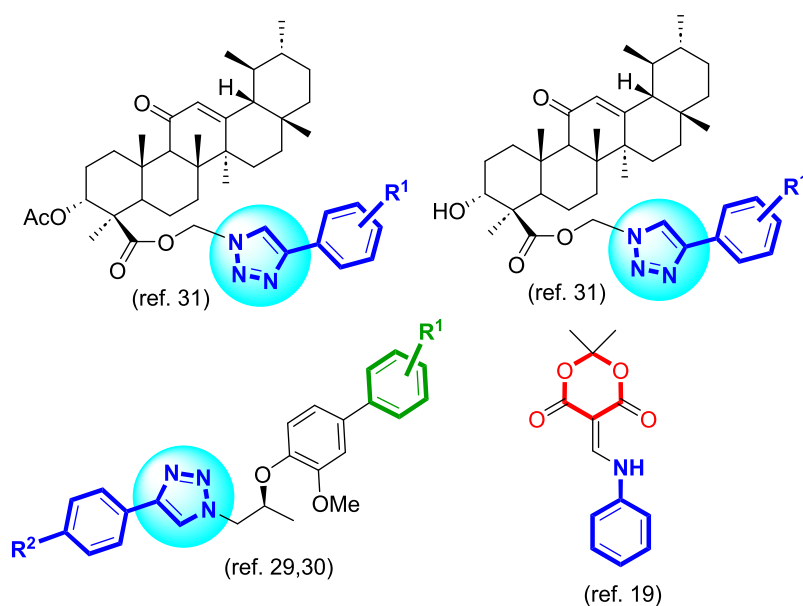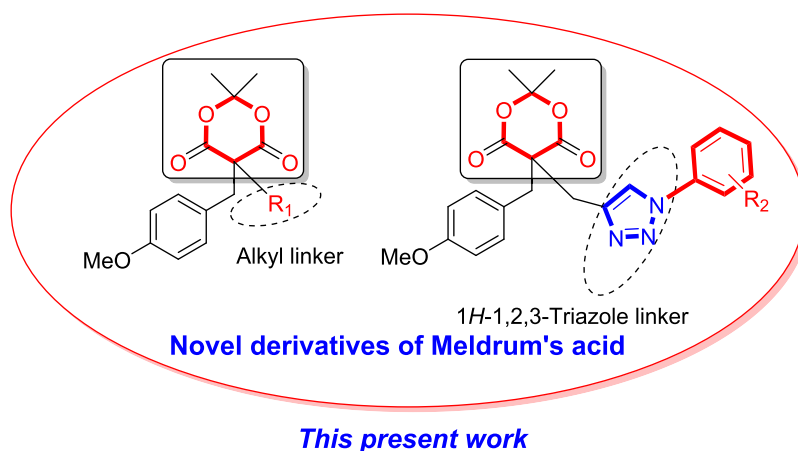
Figure 2. Rational design of the current study.

Scheme 2. Reagents and Conditions: (a) Pyridine, Room Temperature, 15 h, 97%; (b) NaBH$_4$, EtOH, 0 °C to Room Temperature, 2−3 h, 98%; and (c) R$_1$-Br (Different Alkyl Bromides, 4a,b), K$_2$CO$_3$, DMF, Room Temperature, 18 h, 96−98% (5a,b)
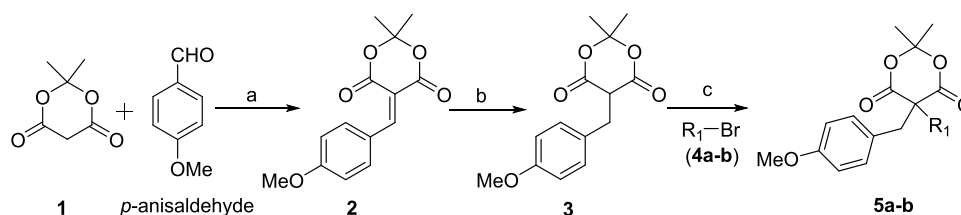

Table 1. Synthesis of Alkyl Derivatives of Meldrum's Acid (5a,b)

reactant	reagent (4a,b)	R$_1$-group	alkyl derivatives of meldrum (5a,b)	yield of (5a,b) (%)[a]
3	4a	propargyl	5a	96
3	4b	benzyl	5b	98

[a]Yields refer to pure isolated products.

the different degrees of activity. The inhibitory action of α-glucosidase is influenced by a wide variety of functional groups, including both electronegative and electropositive ones.

3.1. In Vitro α-Glucosidase Inhibition. To investigate the pharmacological importance of these synthesized molecules, all the hybrids were evaluated for their antidiabetic capability by inhibiting α-glucosidase. The parent compound (**1**) along with compounds **2−3** and **5a** was not able to inhibit
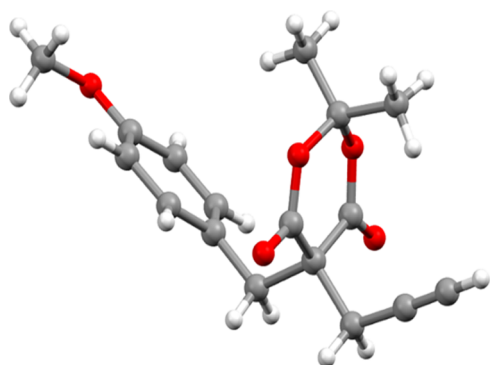
Figure 3. X-ray crystal structure of **5a**.

Table 2. Synthesis of 1*H*-1,2,3-Triazole Derivatives of Meldrum's Acid (7a−k)

reactant	R₂-Group	1*H*-1,2,3-triazole derivatives of meldrum's acid (**7a−k**)	yield of (**7a−k**) (%)[a]
5a	Ph	**7a**	96
5a	2-MeC$_6$H$_4$	**7b**	98
5a	2-MeOC$_6$H$_4$	**7c**	98
5a	2-F$_3$CC$_6$H$_4$	**7d**	96
5a	4-MeOC$_6$H$_4$	**7e**	98
5a	3-F$_3$CC$_6$H$_4$	**7f**	96
5a	3-BrC$_6$H$_4$	**7g**	97
5a	4-BrC$_6$H$_4$	**7h**	97
5a	4-ClC$_6$H$_4$	**7i**	96
5a	4-FC$_6$H$_4$	**7j**	97
5a	4-F$_3$CC$_6$H$_4$	**7k**	96

[a]Yields refer to pure isolated products.

α-glucosidase (above 50%) and thus considered inactive; however, compound **5b** exhibited notable inhibition with the addition of R$_1$-benzyl (IC$_{50}$ = 80.21 ± 0.75 μM), as compared to acarbose (IC$_{50}$ = 873.34 ± 1.67 μM) (Figure 6).

Figure 7 shows compounds 7a−k with similar R-groups like Scheme 1 compounds, while R$_1$-propargyl is converted into triazole, which is constant and R$_2$ is varied among all members, which determine the importance of different groups in the inhibition of α-glucosidase. For instance, **7a**, with the addition of R$_2$-phenyl, exhibited several times potent anti-α-glucosidase activity (IC$_{50}$ = 46.43 ± 0.72 μM), as compared to acarbose (a marketed drug with IC$_{50}$ = 873.34 ± 1.67 μM). In compound **7b**, the substitution of R$_2$-2-MeC$_6$H$_4$ further enhanced the antidiabetic capability with an IC$_{50}$ value of 20.61 ± 0.35 μM, as compared to **7a**. On the other hand, the addition of 2-MeOC$_6$H$_4$ in **7c** slightly reduced the α-glucosidase inhibition (IC$_{50}$ = 27.82 ± 0.31 μM), as compared to **7b**. Like **7b** and **7c**, a slight decline in the α-glucosidase inhibition was observed for **7d−7f** upon addition of 2-F$_3$CC$_6$H$_4$, 4-MeOC$_6$H$_4$, and 3-F$_3$CC$_6$H$_4$ with IC$_{50}$ values of 37.04 ± 0.51, 39.86 ± 0.68, and 41.42 ± 0.53 μM, respectively. However, the substitution of 3-BrC$_6$H$_4$ and 4-BrC$_6$H$_4$ in **7g** and **7h**, respectively, resulted in improved antidiabetic potential with IC$_{50}$ values of 32.19 ± 0.27 and 29.62 ± 0.17 μM, respectively, as compared to **7b** and **7c**. In contrast, the addition of 4-ClC$_6$H$_4$ in **7i** interestingly increased the α-glucosidase inhibitory potency of **7i** (IC$_{50}$ = 4.63 ± 0.11 μM) and turned it to be the most potent antidiabetic agent among other members of this series, whereas the addition of 4-FC$_6$H$_4$ in **7j** decreased the antidiabetic property of **7j** (IC$_{50}$ = 23.98 ± 0.65 μM), as compared to **7i**. Moreover, the incorporation of 4-F$_3$CC$_6$H$_4$ in **7k** further declined its biological activity (IC$_{50}$ = 28.52 ± 0.34 μM), even though **7k** exhibited a several-fold more potent anti-α-glucosidase effect as compared to acarbose. Overall, the structure−activity relationship revealed that the triazole basic skeleton is the key component for the anti-α-glucosidase

activity, while different R$_2$ attached groups are also responsible for their varied inhibitory activities. The structure−activity relationship (SAR) of these compounds is depicted in Figure 7.

3.2. Molecular Docking Studies. We have performed docking studies of active analogues including **5b** and **7a−k** to determine their binding strength with the active site residues of α-glucosidase. Preceding to the docking of our active hits, we redocked the cocrystalized ligand (competitive inhibitor maltose) in the active site of the enzyme−ligand complex to validate the docking procedure. The redocking results showed excellent superimposition of the docked conformation of maltose on its cocrystalized conformation with a root-mean-square deviation (RMSD) value of 0.32 Å and docking score of −6.66 kcal/mol. The known inhibitor binds with the catalytic triad (Asp215, Glu277, and Asp352). In addition, it also forms interactions with Asp69, His112, Arg213, His351, and Arg442. It indicates that the docking method can correctly identify the binding modes of newly synthesized ligands.

Molecular docking clearly demonstrates the pattern of ligand binding in the active site of the enzyme, which reflects the reason of their varied inhibitory potency and correlates with the experimental results. We observed that the Meldrum moiety of the compounds plays an important role in binding with the active site residues, whereas the methoxy-substituted phenyl ring is fitted in the core of the active site, while the triazole-substituted R$_2$ group resides at the entrance loop of the active site. The docked orientations of all the compounds are shown in Figure 8.

The binding mode of the most active compound, **7i**, better explains its higher inhibitory potential; the Meldrum moiety of **7i** fits beneath the core of the active site between Glu277, Gln279, Phe303, Asp352, Gln353, Glu411, and Arg442. The ligand does not directly interact with the residues of the catalytic triad (Asp215, Glu277, and Asp352), which is

Scheme 3. Reagents and Conditions: (a) R$_2$−N$_3$ (different substituted aromatic azides, 6a−k), CuI, Et$_3$N, CH$_3$CN, Room Temperature, 3 h, and 7a−k (96−98%)
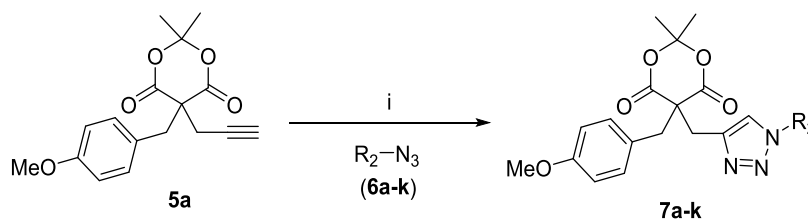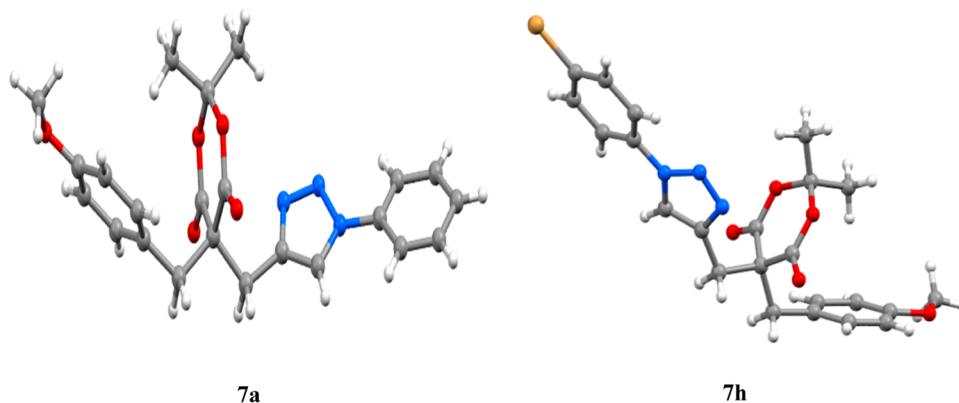
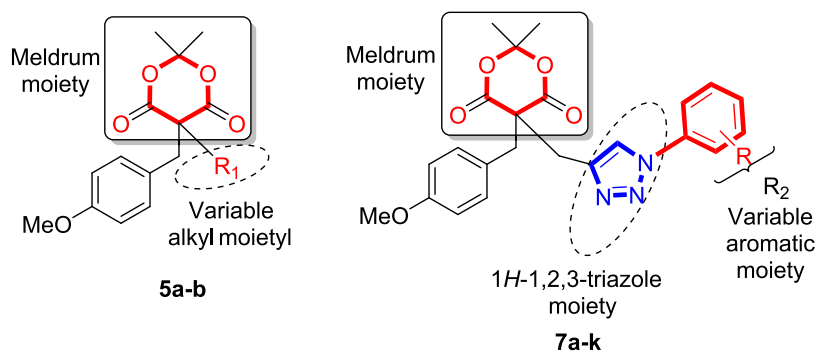**Figure 4.** X-ray crystal structures of compounds **7a** and **7h**.

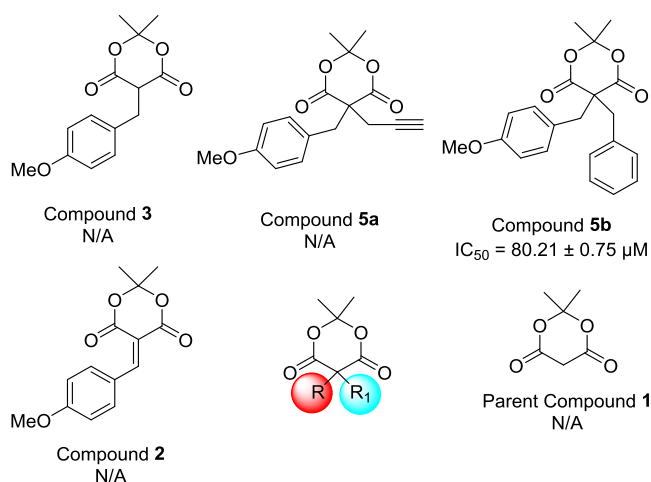**Figure 5.** General structural feature of the synthesized Meldrum's acid derivatives.

Figure 6. In vitro α-glucosidase inhibition of Meldrum acid's derivatives (**1−5b**).

acceptable that the Meldrum moiety cannot form hydrogen bonds (H-bonds) with those acidic residues. However, the Meldrum of **7i** mediates strong H-bonds with the side chains of the Gln279 and Arg442 at 3.06 and 3.08 Å, respectively. The Meldrum-substituted methoxyphenyl ring of **7i** fits well at the hydrophobic groove above the core of the active site, which is composed of Tyr72, Val109, His112, Tyr158, Phe159, Phe178, Gln182, and Val216. The triazole moiety of the compound did not form any hydrophilic interaction with the active site due to its small size and expanded nature of the entrance loop and however fitted well in between several residues (Asp242, His280, Thr306, Asp307, Thr310, Ser311, Pro312, and Arg315) at the entrance of the active site. The binding mode of **7i** is shown in Figure 9. The compound **7i** exhibited −8.62 kcal/mol docking score (DS), which is higher than the DS of all the compounds; it also validates the experimental findings (Table 3).

The docked conformations of the rest of the compounds were compared with the docked conformation of **7i** to understand the SAR of all the compounds. It was observed that the Meldrum ring and the methoxyphenyl ring of the second most active compounds (**7b**, **7j**, and **7c**) adopted almost similar orientations like **7i**; however, the triazole ring and its substituted R_2 moiety of these compounds drastically changed conformation because of the expanded surface of the active site entrance. Due to this conformational change, the Meldrum group of **7b**, **7j**, and **7c** formed only single H-bonds with the side chain of Gln279 and lost one H-bond with Arg442; consequently, their activity was considerably declined as compared to **7i**. This is also evident with their docking scores. These compounds exhibited a DS in the range of −6.90 to −6.44 kcal/mol, which is less than the docking score of **7i**. The same binding pattern was followed by compounds **7h**, **7g**, **7d**, and **7e**. In addition to the H-bond with Gln279, compounds **7h**, **7g**, and **7e** also formed hydrophobic interactions with Tyr158, Arg315, and Phe178, respectively.

When the binding mode of **7k** was compared with the docking conformation of **7i**, we observed that the triazole and the R_2 of **7k** took almost similar binding modes like **7i**; however, its Meldrum moiety was tilted around 45° from the meldrum of **7i**; as a result, the interaction of its Meldrum with Gln279 and Arg442 is totally lost. Due to this conformational variation, the methoxyphenyl ring of **7k** was tilted toward Glu277 and Arg213, where the side chain of Arg213 provided
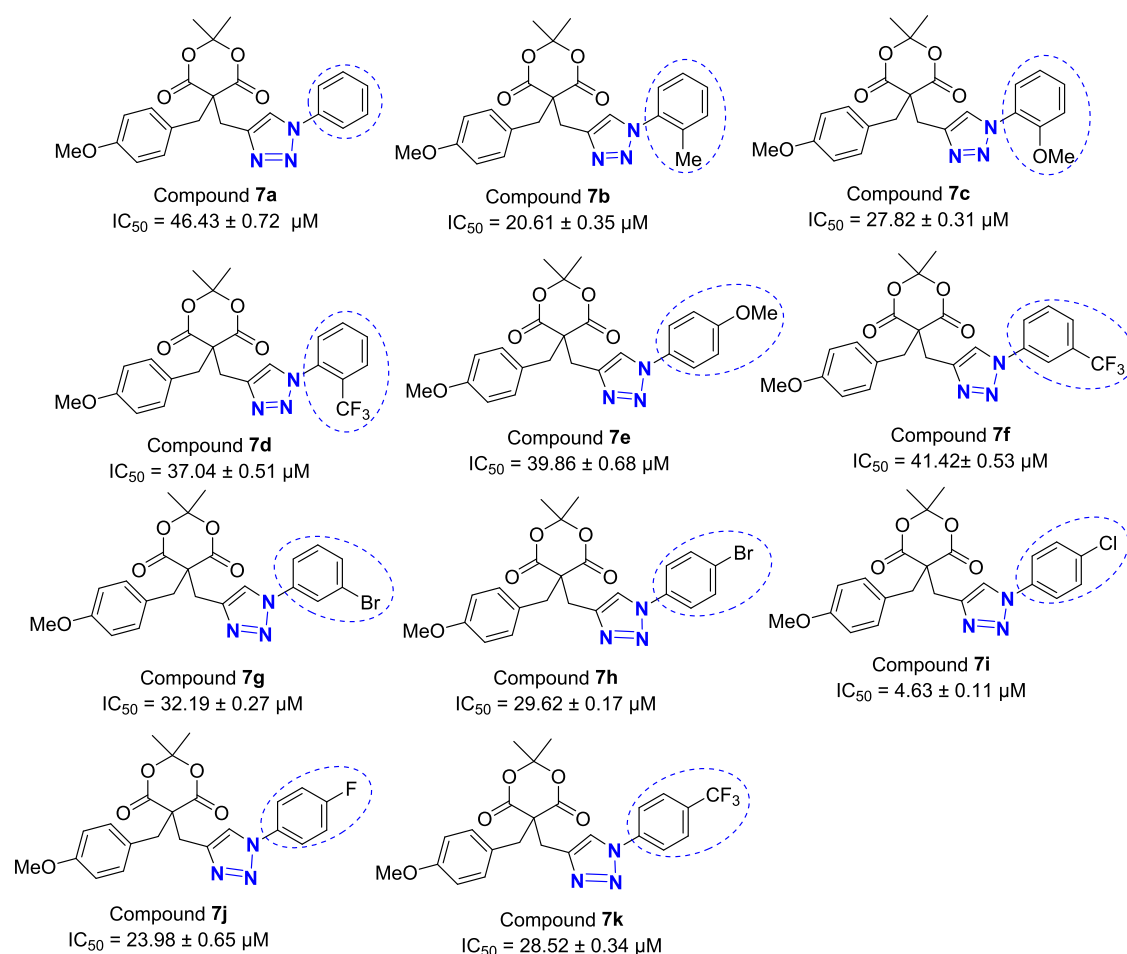
Figure 7. In vitro α-glucosidase inhibition and SAR of Meldrum's acid derivatives (**7a–k**).

H-bonds to the methoxy oxygen of **7k**. Interestingly, the ligand **7f** was found deeply inserted inside the active site; as a result, its Meldrum moiety fits in the hydrophobic groove instead of the core of the active site, and its R_2 group was placed at a position where the Meldrum ring of other compounds is fitted. Therefore, the Meldrum of **7f** lost interactions with Glu279 or Arg442 and only stabilized through H-bonds with the side chain of Arg213, while its triazole ring or R_2 moiety did not form any interaction. This huge conformational difference was responsible for the further decrease of the biological activity of **7f** as compared to **7i**. The binding mode of **7a** was found to be considerably like the docking conformation of **7f** that further validates their similar range of inhibitory affinity. However, its Meldrum moiety was tilted toward Arg442 and mediates a H-bond with the side chain of Arg442. Similarly, the docking conformation of **5b**, the least active compound, was compared with that of **7i**, which revealed that the Meldrum moiety of **5b** mediated only a single H-bond with the side chain of Gln279 but lost bonding with Arg442 or other surrounding residues.

With the docking studies, it was identified that the triazole and its substituted R_2 group do not mediate interaction with active site residues but produce conformational changes in compounds, which affect the binding of the Meldrum moiety of compounds with the residues, more specifically Glu279 and Arg442 that play crucial roles in ligand stability. The docking scores and atom-based protein−ligand interactions of all the docked compounds are given in Table 3. The docking results indicate that the known inhibitor (maltose) binds with the

catalytic triad (Asp215, Glu277, and Asp352) and mediates H-bonds with Asp69, His112, Arg213, His351, and Arg442, while our ligands interact primarily with Gln279, Arg213, and Arg442.

4. CONCLUSIONS

The "click" chemistry was utilized in a highly efficient manner to synthesize a series of novel alkyl derivatives (**2−5a,b**) and 1*H*-1,2,3-triazole derivatives (**7a−k**) of Meldrum's acid. The structures of the synthesized molecules were characterized, and those were screened for in vitro α-glucosidase inhibitory activity. Among all the tested compounds, **7i** displayed highly potent inhibitory activity and was found to be several times more potent than acarbose. Furthermore, the binding pattern of the active molecules was examined through molecular docking, which revealed that the Meldrum moiety is the main constituent and essential part for interaction with active site residues; however, the triazole-substituted R_2 group variably changes the position and causes conformational changes that influence the binding of the Meldrum moiety; as a result, the inhibitory potency of compounds is changed.

5. EXPERIMENTAL SECTION

5.1. General. All reagents were obtained from Sigma-Aldrich, Germany. The silica gel for column chromatography was 100−200-mesh. Solvents were purified by following standard procedures. The high-resolution electrospray ionization mass spectra (HR-ESI-MS) were recorded on an Agilent
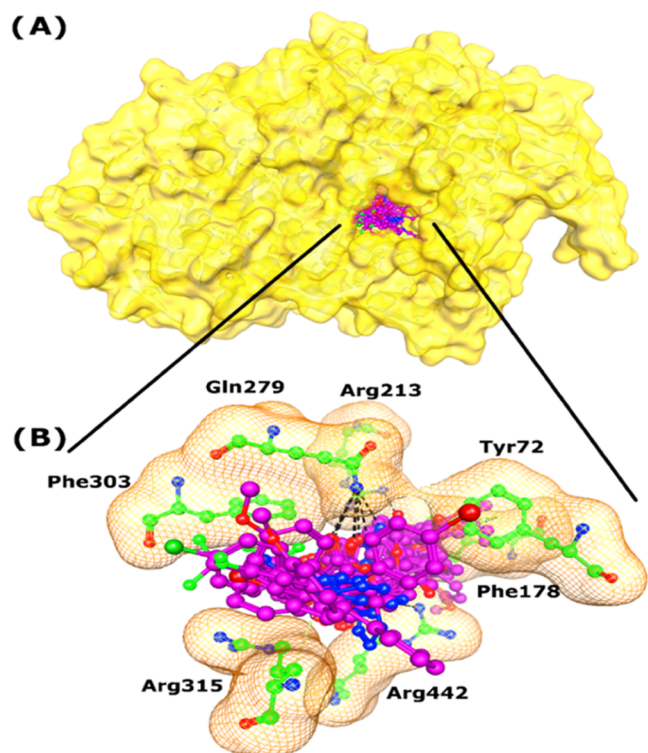
Figure 8. (A) Docked conformations of compounds (shown in the magenta ball and stick model) are shown in the active site of the α-glucosidase enzyme (presented in the yellow surface model). (B). Binding interactions of ligands with the active site residues are shown. Only those residues which are involved in the H-bonding or hydrophobic interactions with ligands are displayed for clarity purpose. The ligand residue H-bonds are depicted in black dashed lines, and hydrophobic interactions are presented in green dashed lines. The interacting residues are shown in the green ball and stick model and in orange surface presentation, while compounds are shown in the magenta ball and stick model.

6530 LC Q-TOF instrument. The ^{1}H and ^{13}C NMR spectra were recorded on a NMR spectrometer (Bruker: 600 MHz for ^{1}H, 150 MHz for ^{13}C and 564 MHz for ^{19}F) using CDCl$_3$ as a solvent. Thin-layer chromatography (TLC) was carried using silica gel F$_{254}$ precoated plates. UV light and I$_2$ stain were used to visualize the spots. Organic extracts and solutions of pure compounds were dried over anhydrous MgSO$_4$. Single crystals of compounds **5a**, **7a**, and **7h** were mounted on a MiTeGen loop with grease and examined on a Bruker D8 Venture APEX diffractometer equipped with a Photon 100 CCD area detector at 296 (2) K using graphite-monochromated Mo Kα radiation (λ = 0.71073 Å). Data were collected using APEX-II software,[38] integrated using SAIN,[39] and corrected for absorption using a multiscan approach (SADABS).[40] Final cell constants were determined from full least squares refinement of all observed reflections. The structures were solved using intrinsic phasing (SHELXT).[41] All non-H atoms were in subsequent difference maps and refined anisotropically. H-atoms were added at calculated positions and refined with a riding model. H atoms on O and N atoms were in a difference map and refined with constrained O−H and N−H distances. The structures of compounds **5a**, **7a**, and **7h** have been deposited with the CCDC (CCDC deposition numbers = 2226650 (**5a**), 2226651 (**7a**), and 2226652 (**7h**)).
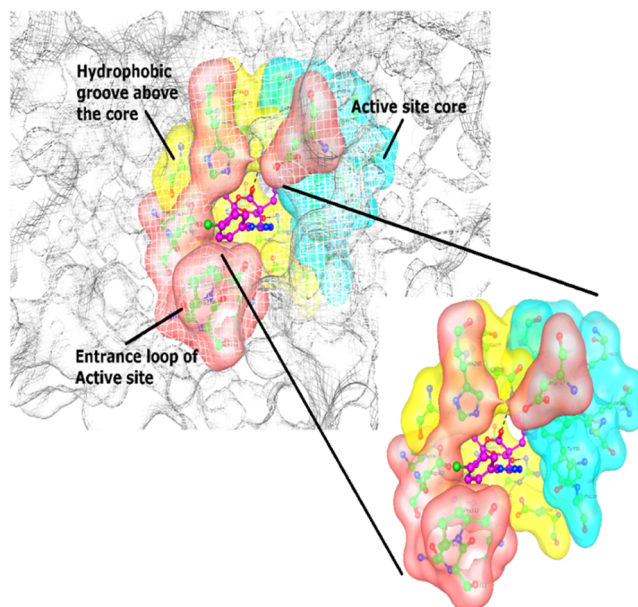
Figure 9. Binding mode of the most active compound (**7i**) is shown in the active site of α-glucosidase with its enhanced view. The entrance loop of the active site is shown in the pink surface model, the active site core is presented in the cyan surface model, and the hydrophobic groove above the core is depicted in the yellow surface presentation. The ligand is presented in the magenta ball and stick model, and H-bonds are shown in black dashed lines.

5.2. Knoevenagel General Procedure for the Synthesis of Compound 2. Meldrum's acid (1.0 equiv) and *p*-anisaldehyde (1.0 equiv) were mixed in pyridine (0.1 M, 10 mL) and stirred at room temperature overnight under a nitrogen atmosphere. The resultant reaction mixture was dried, and the solids were either employed directly without additional purification or recrystallized in MeOH to produce pure compound **2** (97%).

5.2.1. 5-(4-Methoxybenzylidene)-2,2-dimethyl-1,3-dioxane-4,6-dione (2). Yellow solid (yellow color crystals); yield = 97%; m.p. 126−128 °C, ^{1}H NMR (600 MHz, chloroform-*d*) δ 8.34 (s, 1H), 8.23−8.15 (m, 2H), 7.02−6.88 (m, 2H), 3.88 (d, *J* = 1.8 Hz, 3H), 1.76 (s, 6H); ^{13}C NMR (150 MHz, CDCl$_3$) δ 164.6, 164.0, 160.4, 157.9, 137.6, 124.7, 114.3, 110.8, 104.1, 55.68, 27.49; HRMS (ESI$^+$): found [M + Na]$^+$: 285.0543 C$_{14}$H$_{14}$O$_5$Na required 285.0541.

5.3. General Procedure for the Synthesis of Compound 3. A stirred solution of the Knoevenagel product (**2**, 1.0 equiv) suspended in absolute EtOH (0.1 M) received portions of sodium borohydride (2.0 equiv) during the course of 2 h. Upon completion, as determined by TLC, the reaction was quenched with 1 M aqueous HCl (15 mL/mmol), and the precipitate was filtered, washed with water, and dried at the pump to yield the desired compound without further purification or recrystallized in MeOH to yield pure compound **3** in a high yield (98%).

5.3.1. 5-(4-Methoxybenzyl)-2,2-dimethyl-1,3-dioxane-4,6-dione (3). White solid; yield = 98%; m.p. 83−85 °C, ^{1}H NMR (600 MHz, chloroform-*d*) δ 7.24−7.16 (m, 2H), 6.84−6.73 (m, 2H), 3.74 (d, *J* = 1.9 Hz, 3H), 3.70 (dt, *J* = 4.8, 2.4 Hz, 1H), 3.43−3.37 (m, 2H), 1.69 (s, 3H), 1.45 (s, 3H); [3]C NMR (150 MHz, CDCl$_3$) δ 165.4, 158.7, 130.9, 129.0, 113.9, 105.1, 55.2, 48.2, 31.4, 28.4, 27.3; HRMS (ESI$^+$): found [M + H]$^+$: 265.0925 C$_{14}$H$_{17}$O$_5$ required 265.0928.

Table 3. Molecular Docking Results of Meldrum's Acid Derivatives[a]

			protein–ligand interaction			
compounds	IC$_{50}$ (μM)	DS (kcal/mol)	ligand atom	receptor atom	interaction	distance
7i	4.63	−8.62	O15	NE2-GLN279	HBA	3.06
			O16	NH1-ARG442	HBA	3.08
7b	20.61	−6.90	O16	NE2-GLN279	HBA	2.90
7j	23.98	−6.83	O15	NE2-GLN279	HBA	3.09
7c	27.82	−6.44	O16	NE2-GLN279	HBA	2.92
7k	28.52	−5.83	O53	NH2-ARG213	HBA	3.01
7h	29.62	−4.51	O16	NE2-GLN279	HBA	3.16
			6-ring	6-ring-TYR158	π−π	3.86
7g	32.19	−4.32	O15	NE2-GLN279	HBA	3.01
			6-ring	CB-ARG315	π-H	3.63
7d	37.04	−3.39	O16	NE2-GLN279	HBA	3.10
7e	39.86	−3.30	O16	NE2-GLN279	HBA	3.09
			C55	6-ring-PHE178	π-H	3.96
7f	41.42	−3.11	O16	NH1-ARG213	HBA	3.49
			O16	NH2-ARG213	HBA	3.38
7a	46.43	−3.09	O16	NH1-ARG442	HBA	2.70
5b	80.21	−2.56	O42	NE2-GLN279	HBA	2.96

[a]DS = docking score, HBA = hydrogen bond acceptor, and HBD = hydrogen bond donor.

5.4. General Procedure for the Synthesis of Compounds 5a and 5b. To a solution of compound **3** (1.0 equiv) in dry DMF (10 mL) were added successively anhydrous potassium carbonate (2.0 equiv) and propargyl bromide or benzyl bromide (1.1 equiv). The reaction mixture was stirred at room temperature for 18 h till completion of the reaction (monitored by TLC analysis). After completion of the reaction, it was extracted with EtOAc (3 × 30 mL). The combined organic layer was dried over anhydrous MgSO$_4$ and concentrated under reduced pressure on a rotary evaporator to furnish the desired compounds without further purification or recrystallized in EtOAc and DCM (1:1) solution to afford pure compounds **5a** (98%) and **5b** (96%), respectively.

5.4.1. 5-(4-Methoxybenzyl)-2,2-dimethyl-5-(prop-2-yn-1-yl)-1,3-dioxane-4,6-dione (5a). Light-green solid (light-green crystals from EtOAc and DCM (1:1) solution); yield = 98%; m.p. 146−148 °C, ^{1}H NMR (600 MHz, chloroform-d) δ 7.04−6.93 (m, 2H), 6.80−6.70 (m, 2H), 3.69 (d, J = 1.9 Hz, 3H), 3.13 (s, 2H), 2.93 (t, J = 2.3 Hz, 2H), 2.10 (d, J = 5.2 Hz, 1H), 1.59 (s, 3H), 0.78 (s, 3H); ^{13}C NMR (150 MHz, CDCl$_3$) δ 167.7, 159.4, 131.1, 126.2, 114.2, 106.5, 78.3, 72.9, 56.9, 55.2, 43.9, 30.2, 28.5, 28.1; HRMS (ESI$^+$): found [M + H]$^+$: 303.2076 C$_{17}$H$_{19}$O$_5$ required 303.2074.

5.4.2. 5-Benzyl-5-(4-methoxybenzyl)-2,2-dimethyl-1,3-dioxane-4,6-dione (5b). Light-yellow solid; yield = 96%; m.p. 142−145 °C, ^{1}H NMR (600 MHz, chloroform-d) δ 7.21 (s, 2H), 7.18−7.16 (m, 1H), 7.13 (d, J = 7.6 Hz, 2H), 7.08−7.05 (m, 2H), 6.76−6.72 (m, 2H), 3.68 (d, J = 2.0 Hz, 3H), 3.36 (s, 2H), 3.33 (s, 2H), 0.65 (s, 3H), 0.58 (s, 3H); ^{13}C NMR (150 MHz, CDCl$_3$) δ 168.2, 159.2, 134.9, 131.2, 130.1, 128.8, 127.7, 126.9, 114.1, 105.8, 60.2, 55.2, 44.8, 44.2, 28.7, 28.5; HRMS (ESI$^+$): found [M + H]$^+$: 355.1160 C$_{21}$H$_{22}$O$_5$ required 355.1163.

5.5. General Procedure for the Synthesis of 1H-1,2,3-Triazol Derivatives of Meldrum's Acid (7a−k). CuI (2.0 equiv) and Et$_3$N (3.0 equiv) were added to a solution of compound **5a** (1.0 equiv) and substituted aromatic azides **6a−k** (1.2 equiv) in acetonitrile (10 mL), and the mixture was stirred for three hours (3 h). The desired compounds were produced without the need for further purification by diluting

the reaction mixture with EtOAc (30 mL), adding 20 mL of aqueous NH$_4$Cl, extracting the aqueous layer with EtOAc (3 × 30 mL), washing the combined organic layer with brine (1 × 20 mL), drying it over anhydrous MgSO$_4$, filtering it, and then concentrating it under reduced pressure on a rotary evaporator to furnish the desired compounds without further purification, or few compounds were recrystallized in EtOAc solution to afford pure 1H-1,2,3-triazol derivatives of Meldrum's acid **7a−k** in high yields (96−98%).

5.5.1. 5-(4-Methoxybenzyl)-2,2-dimethyl-5-((1-phenyl-1H-1,2,3-triazol-4-yl)methyl)-1,3-dioxane-4,6-dione (7a). Brown solid (brown crystals from EtOAc solvent); yield = 96%; m.p. 174−176 °C, ^{1}H NMR (600 MHz, chloroform-d) δ 7.79 (s, 1H), 7.67−7.62 (m, 2H), 7.48 (dd, J = 8.6, 7.1 Hz, 2H), 7.43−7.38 (m, 1H), 7.16−7.12 (m, 2H), 6.83−6.79 (m, 2H), 3.74 (s, 3H), 3.63 (s, 2H), 3.38 (s, 2H), 1.39 (s, 3H), 0.72 (s, 3H); ^{13}C NMR (150 MHz, CDCl$_3$) δ 168.2, 159.5, 142.5, 136.8, 131.4, 129.8, 128.9, 126.4, 120.6, 114.3, 106.8, 56.8, 55.3, 45.0, 34.2, 28.9, 28.6; HRMS (ESI$^+$): found [M + H]$^+$: 422.1734 C$_{23}$H$_{24}$N$_3$O$_5$ required 422.1732.

5.5.2. 5-(4-Methoxybenzyl)-2,2-dimethyl-5-((1-(o-tolyl)-1H-1,2,3-triazol-4-yl)methyl)-1,3-dioxane-4,6-dione (7b). Red solid; yield = 98%; m.p. 146−148 °C, ^{1}H NMR (600 MHz, chloroform-d) δ 7.61−7.39 (m, 1H), 7.33 (tq, J = 25.4, 8.7, 7.4 Hz, 3H), 7.24−7.01 (m, 3H), 6.80 (dq, J = 16.8, 10.2, 9.5 Hz, 2H), 3.74 (t, J = 7.7 Hz, 3H), 3.53−3.28 (m, 2H), 3.22−3.13 (m, 1H), 2.24−2.13 (m, 2H), 1.38 (d, J = 18.2 Hz, 2H), 1.30−1.17 (m, 3H), 0.71 (d, J = 12.7 Hz, 3H); ^{13}C NMR (150 MHz, CDCl$_3$) δ 168.2, 159.5, 141.6, 133.5, 131.4, 131.2, 126.8, 126.4, 125.8, 124.1, 114.3, 106.7, 57.0, 55.3, 44.9, 34.3, 28.9, 28.7, 28.5, 17.8; HRMS (ESI$^+$): found [M + H]$^+$: 436.1886 C$_{24}$H$_{26}$N$_3$O$_5$ required 436.1888.

5.5.3. 5-(4-Methoxybenzyl)-5-((1-(2-methoxyphenyl)-1H-1,2,3-triazol-4-yl)methyl)-2,2-dimethyl-1,3-dioxane-4,6-dione (7c). Dark-brown solid; yield = 98%; m.p. 152−155 °C, ^{1}H NMR (600 MHz, Chloroform-d) δ 7.90 (s, 1H), 7.65 (dd, J = 7.7, 1.7 Hz, 1H), 7.38 (td, J = 7.9, 1.7 Hz, 1H), 7.15−7.12 (m, 2H), 7.04 (t, J = 7.9 Hz, 2H), 6.82−6.79 (m, 2H), 3.84 (s, 3H), 3.74 (s, 3H), 3.63 (s, 2H), 3.38 (s, 2H), 1.34 (s, 3H), 0.72 (s, 3H); ^{13}C NMR (150 MHz, CDCl$_3$) δ 168.2, 159.4,

151.1, 141.0, 131.3, 130.1, 126.5, 126.1, 125.4, 124.6, 121.1, 114.2, 112.1, 106.6, 57.1, 55.8, 55.3, 44.9, 34.3, 28.7, 28.6; HRMS (ESI$^+$): found [M + H]$^+$: 452.1841 $C_{24}H_{26}N_3O_6$ required 452.1843.

5.5.4. 5-(4-Methoxybenzyl)-2,2-dimethyl-5-((1-(2-(trifluoromethyl)phenyl)-1H-1,2,3-triazol-4-yl)methyl)-1,3-dioxane-4,6-dione (7d). Red solid; yield = 96%; m.p. 154−57 °C, ^{1}H NMR (600 MHz, chloroform-*d*) δ 7.83−7.79 (m, 1H), 7.72−7.61 (m, 3H), 7.43 (d, *J* = 7.8 Hz, 1H), 7.15−7.10 (m, 2H), 6.80 (dq, *J* = 8.6, 3.0 Hz, 2H), 3.73 (s, 3H), 3.62 (s, 2H), 3.38 (s, 2H), 1.35 (s, 3H), 0.71 (s, 3H); ^{13}C NMR (150 MHz, CDCl$_3$) δ 168.1, 159.5, 141.8, 133.1, 131.4, 130.5, 128.9, 126.4, 125.5, 117.4, 114.3, 106.7, 57.1, 55.3, 45.0, 34.1, 28.9, 28.6; ^{19}F NMR (564 MHz, chloroform-*d*) δ −59.1; HRMS (ESI$^+$): found [M + H]$^+$: 490.1624 $C_{24}H_{23}F_3N_3O_5$ required 490.1626.

5.5.5. 5-(4-Methoxybenzyl)-5-((1-(4-methoxyphenyl)-1H-1,2,3-triazol-4-yl)methyl)-2,2-dimethyl-1,3-dioxane-4,6-dione (7e). Light-brown solid; yield = 98%; m.p. 182−185 °C, ^{1}H NMR (600 MHz, chloroform-*d*) δ 7.74 (s, 1H), 7.58−7.55 (m, 2H), 7.18−7.15 (m, 2H), 7.02−6.98 (m, 2H), 6.86−6.83 (m, 2H), 3.86 (s, 3H), 3.77 (s, 3H), 3.65 (s, 2H), 3.41 (s, 2H), 1.43 (s, 3H), 0.75 (s, 3H); ^{13}C NMR (150 MHz, CDCl$_3$) δ 168.1, 159.8, 159.4, 142.2, 131.3, 130.2, 126.4, 122.1, 120.7, 114.7, 114.2, 106.7, 56.7, 55.6, 55.2, 45.0, 34.1, 28.8, 28.6; HRMS (ESI$^+$): found [M + H]$^+$: 452.1831 $C_{24}H_{26}N_3O_6$ required 452.1828.

5.5.6. 5-(4-Methoxybenzyl)-2,2-dimethyl-5-((1-(3-(trifluoromethyl)phenyl)-1H-1,2,3-triazol-4-yl)methyl)-1,3-dioxane-4,6-dione (7f). Dark-brown solid; yield = 96%; m.p. 142−145 °C, ^{1}H NMR (600 MHz, chloroform-*d*) δ 7.94 (d, *J* = 1.9 Hz, 1H), 7.87 (d, *J* = 7.7 Hz, 2H), 7.68−7.61 (m, 2H), 7.15−7.10 (m, 2H), 6.84−6.79 (m, 2H), 3.74 (s, 3H), 3.63 (s, 2H), 3.38 (s, 2H), 1.42 (s, 3H), 0.72 (s, 3H); ^{13}C NMR (150 MHz, CDCl$_3$) δ 168.1, 159.5, 137.1, 131.3, 130.5, 126.2, 125.4, 123.5, 120.5, 117.3, 114.3, 106.8, 56.5, 55.2, 45.0, 34.0, 28.8, 28.5; ^{19}F NMR (564 MHz, chloroform-*d*) δ −62.87; HRMS (ESI$^+$): found [M + H]$^+$: 490.1592 $C_{24}H_{23}F_3N_3O_5$ required 490.1594.

5.5.7. 5-((1-(3-Bromophenyl)-1H-1,2,3-triazol-4-yl)methyl)-5-(4-methoxybenzyl)-2,2-dimethyl-1,3-dioxane-4,6-dione (7g). Red solid; yield = 97%; m.p. 176−179 °C, ^{1}H NMR (600 MHz, chloroform-*d*) δ 7.89 (t, *J* = 2.0 Hz, 1H), 7.83 (s, 1H), 7.63 (ddd, *J* = 8.1, 2.1, 0.9 Hz, 1H), 7.57 (ddd, *J* = 8.0, 1.9, 0.9 Hz, 1H), 7.39 (t, *J* = 8.1 Hz, 1H), 7.18−7.15 (m, 2H), 6.87−6.84 (m, 2H), 3.78 (s, 3H), 3.66 (s, 2H), 3.41 (s, 2H), 1.44 (s, 3H), 0.76 (s, 3H); ^{13}C NMR (150 MHz, CDCl$_3$) δ 168.1, 159.5, 137.7, 131.9, 131.3, 131.1, 126.3, 123.6, 123.3, 119.0, 114.3, 106.9, 56.6, 55.3, 45.0, 34.1, 28.9, 28.6; HRMS (ESI$^+$): found [M]$^+$: 500.0711 $C_{23}H_{22}^{79}BrN_3O_5$ required 500.0713. Found [M]$^+$: 502.0694 $C_{23}H_{22}^{81}BrN_3O_5$ required 502.0692.

5.5.8. 5-((1-(4-Bromophenyl)-1H-1,2,3-triazol-4-yl)methyl)-5-(4-methoxybenzyl)-2,2-dimethyl-1,3-dioxane-4,6-dione (7h). Light-brown solid; yield = 97%; m.p. 178−181 °C, ^{1}H NMR (600 MHz, chloroform-*d*) δ 7.78 (s, 1H), 7.61−7.57 (m, 2H), 7.55−7.52 (m, 2H), 7.12−7.09 (m, 2H), 6.81−6.78 (m, 2H), 3.72 (s, 3H), 3.60 (s, 2H), 3.36 (s, 2H), 1.38 (s, 3H), 0.70 (s, 3H); ^{13}C NMR (151 MHz, CDCl$_3$) δ 168.1, 159.4, 135.7, 132.9, 131.3, 126.3, 122.5, 121.8, 120.4, 114.2, 106.8, 56.5, 55.3, 45.0, 34.0, 29.6, 28.8, 28.6; HRMS (ESI$^+$): found [M]$^+$: 500.0762 $C_{23}H_{22}^{79}BrN_3O_5$ required 500.0760. Found [M]$^+$: 502.0745 $C_{23}H_{22}^{81}BrN_3O_5$ required 502.0748.

5.5.9. 5-((1-(4-Chlorophenyl)-1H-1,2,3-triazol-4-yl)methyl)-5-(4-methoxybenzyl)-2,2-dimethyl-1,3-dioxane-4,6-dione (7i). Light-green solid; yield = 96%; m.p. 184−186 °C, ^{1}H NMR (600 MHz, chloroform-*d*) δ 7.77 (s, 1H), 7.62−7.56 (m, 2H), 7.47−7.41 (m, 2H), 7.13−7.09 (m, 2H), 6.82−6.78 (m, 2H), 3.73 (s, 3H), 3.60 (s, 2H), 3.36 (s, 2H), 1.39 (s, 3H), 0.71 (s, 3H); ^{13}C NMR (150 MHz, CDCl$_3$) δ 168.1, 159.4, 142.8, 135.2, 134.6, 131.3, 129.9, 126.3, 121.6, 120.4, 114.2, 106.8, 56.5, 55.3, 45.0, 34.0, 28.8, 28.6; HRMS (ESI$^+$): found [M + H]$^+$: 456.1312 $C_{23}H_{23}ClN_3O_5$ required 456.1310.

5.5.10. 5-((1-(4-Fluorophenyl)-1H-1,2,3-triazol-4-yl)methyl)-5-(4-methoxybenzyl)-2,2-dimethyl-1,3-dioxane-4,6-dione (7j). Light-yellow solid; yield = 97%; m.p. 163−166 °C, ^{1}H NMR (600 MHz, chloroform-*d*) δ 7.75 (s, 1H), 7.65−7.59 (m, 2H), 7.18−7.14 (m, 2H), 7.11 (s, 2H), 6.80 (d, *J* = 8.3 Hz, 2H), 3.73 (s, 3H), 3.61 (s, 2H), 3.36 (s, 2H), 1.40 (s, 3H), 0.71 (s, 3H); ^{13}C NMR (150 MHz, CDCl$_3$) δ 168.1, 159.4, 142.7, 133.1, 131.3, 126.3, 122.5, 120.7, 116.8, 116.6, 114.2, 106.8, 56.5, 55.2, 45.0, 34.1, 29.6, 28.8, 28.6; ^{19}F NMR (564 MHz, chloroform-*d*) δ −111.89; HRMS (ESI$^+$): found [M + H]$^+$: 440.1623 $C_{23}H_{23}FN_3O_5$ required 440.1625.

5.5.11. 5-(4-Methoxybenzyl)-2,2-dimethyl-5-((1-(4-(trifluoromethyl)phenyl)-1H-1,2,3-triazol-4-yl)methyl)-1,3-dioxane-4,6-dione (7k). Light-brown solid; m.p. 178−181 °C, ^{1}H NMR (600 MHz, chloroform-*d*) δ 7.88 (s, 1H), 7.81 (d, *J* = 8.4 Hz, 2H), 7.74 (d, *J* = 8.3 Hz, 2H), 7.11 (d, *J* = 8.3 Hz, 2H), 6.80 (d, *J* = 8.3 Hz, 2H), 3.73 (s, 3H), 3.62 (s, 2H), 3.37 (s, 2H), 1.40 (s, 3H), 0.71 (s, 3H); ^{13}C NMR (150 MHz, CDCl$_3$) δ 168.0, 159.5, 143.1, 139.1, 131.3, 127.0, 126.2, 120.4, 114.2, 106.8, 56.5, 55.2, 45.0, 34.0, 29.6, 28.8, 28.5; ^{19}F NMR (564 MHz, chloroform-*d*) δ −62.64; HRMS (ESI$^+$): found [M + H]$^+$: 490.1599 $C_{24}H_{23}F_3N_3O_5$ required 490.1597.

5.6. α-Glucosidase Inhibition Assay. The recent studies were carried out using methodologies that we have previously published.[42] The substrate *P*-nitro phenyl-α-D-glucopyranoside and enzyme α-glucosidase were dissolved in similar phosphate buffer (pH 6.8), and this buffer, 135 μL/well, was also employed in a 96-well plate as a reaction buffer. The tested compounds, 20 μL/well (0.5 mM) and 20 μL/well enzyme (0.02 U/well), were also added, followed by 15 min of incubation at 37 °C. On the completion of incubation time, 25 μL/well substrate *p*-nitro phenyl-α-D-glucopyranoside was loaded into a 96-well plate for 30 min; changes in absorbance owing to substrate degradation were observed at 400 nm. Acarbose was used as a positive control, and 7% DMSO served as a negative control. Later, statistical analysis was performed on SoftMax Pro suite and Excel to obtain the results for antidiabetic impact of the offered tested materials. The formula given below was used to calculate the percent inhibition of all the tested samples.

$$\%\text{Inhibition} = 100 - \left(\frac{\text{O. D}_{\text{test compound}}}{\text{O. D}_{\text{control}}} \right) \times 100 \tag{1}$$

For all the substances studied, EZ-FIT (Perrella Scientific, Inc., USA) was used to calculate IC$_{50}$. All studies were done in triplicate to avoid predicted mistakes, and differences in the results are reported as standard error of mean values (SEM).

$$\text{SE} = \frac{\sigma}{\sqrt{n}} \tag{2}$$

5.7. Molecular Docking. The crystal structure of isomaltase from Saccharomyces cerevisiae in complex with its competitive inhibitor maltose (PDB code 3A4A)[43] was taken for docking studies. In silico analysis was performed on Molecular Operating Environment (MOE version 2020.09),[44] after validation of its docking protocol. The enzyme file was prepared for docking by adding missing hydrogen atoms and assigning partial charges according to MOE's Amber10: EHT force field. The structures of the compounds were drawn on MOE and saved in the MOE compound database, where the saved structures were minimized using the same force field until the RMS gradient of 0.1 kcal/mol/Å was obtained. During the minimization process, partial charges were calculated automatically. The triangle matcher docking algorithm and London dG scoring function of MOE were used during ligand placement and scoring.

■ ASSOCIATED CONTENT

Ⓢ Supporting Information

The Supporting Information is available free of charge at https://pubs.acs.org/doi/10.1021/acsomega.3c01291.

^{1}H-NMR ^{13}C-NMR, ^{19}F-NMR, and mass spectra of compounds **2, 3, 5a, 5b,** and **7a−7k** (PDF)

■ AUTHOR INFORMATION

Corresponding Authors

Ajmal Khan − *Natural and Medical Sciences Research Center, University of Nizwa, 616 Nizwa, Sultanate of Oman;* ⓞ orcid.org/0000-0001-7851-6080; Email: ajmalkhan@unizwa.edu.om

Ahmed Al-Harrasi − *Natural and Medical Sciences Research Center, University of Nizwa, 616 Nizwa, Sultanate of Oman;* ⓞ orcid.org/0000-0002-0815-5942; Phone: +968 25446328; Email: aharrasi@unizwa.edu.om

Ali Rostami − *Natural and Medical Sciences Research Center, University of Nizwa, 616 Nizwa, Sultanate of Oman;* ⓞ orcid.org/0000-0003-3250-6869; Email: arostami@unizwa.edu.om

Authors

Satya Kumar Avula − *Natural and Medical Sciences Research Center, University of Nizwa, 616 Nizwa, Sultanate of Oman;* ⓞ orcid.org/0000-0003-3941-7164

Saeed Ullah − *Natural and Medical Sciences Research Center, University of Nizwa, 616 Nizwa, Sultanate of Oman*

Sobia Ahsan Halim − *Natural and Medical Sciences Research Center, University of Nizwa, 616 Nizwa, Sultanate of Oman*

Muhammad U. Anwar − *Natural and Medical Sciences Research Center, University of Nizwa, 616 Nizwa, Sultanate of Oman;* ⓞ orcid.org/0000-0003-4740-5737

René Csuk − *Organic Chemistry, Martin-Luther-University Halle-Wittenberg, D-06120 Halle (Saale), Germany;* ⓞ orcid.org/0000-0001-7911-290X

Complete contact information is available at:
https://pubs.acs.org/10.1021/acsomega.3c01291

Notes

The authors declare no competing financial interest.

■ REFERENCES

(1) Kausar, N.; Ullah, S.; Khan, M. A.; Zafar, H.; Atia-tul-Wahab; Choudhary, M. I.; Yousuf, S. Celebrex Derivatives: Synthesis, α-Glucosidase Inhibition, Crystal Structures and Molecular Docking Studies. *Bioorg. Chem.* **2021**, *106*, No. 104499.

(2) Akhter, S.; Ullah, S.; Yousuf, S.; Atia-tul-Wahab; Siddiqui, H.; Choudhary, M. I. Synthesis, Crystal Structure and Hirshfeld Surface Analysis of Benzamide Derivatives of Thiourea as Potent Inhibitors of α-Glucosidase in-Vitro. *Bioorg. Chem.* **2021**, *107*, No. 104531.

(3) Sohrabi, M.; Binaeizadeh, M. R.; Iraji, A.; Larijani, B.; Saeedi, M.; Mahdavi, M. A Review on α-Glucosidase Inhibitory Activity of First Row Transition Metal Complexes: A Futuristic Strategy for Treatment of Type 2 Diabetes. *RSC Adv.* **2022**, *12*, 12011−12052.

(4) Ullah, S.; Mirza, S.; Salar, U.; Hussain, S.; Javaid, K.; Khan, M. K.; Khalil, R.; Atia-tul-Wahab; Ul-Haq, Z.; Perveen, S.; Choudhary, I. M. 2-Mercapto Benzothiazole Derivatives: As Potential Leads for the Diabetic Management. *Med. Chem.* **2020**, *16*, 826−840.

(5) Jaffery, S. M. F.; Khan, M. A.; Ullah, S.; Atia-tul-Wahab; Choudhary, M. I.; Basha, F. Z. Synthesis of New Valinol-Derived Sultam Triazoles as α-Glucosidase Inhibitors. *ChemistrySelect* **2021**, *6*, 9780−9786.

(6) Siddiqui, H.; Baheej, M. A. A.; Ullah, S.; Rizvi, F.; Iqbal, S.; Haniffa, H. M.; Wahab, A.-T.; Choudhary, M. I. Synthesis of 1,2,3,Triazole Modified Analogues of Hydrochlorothiazide via Click Chemistry Approach and in-Vitro α-Glucosidase Enzyme Inhibition Studies. *Mol. Diversity* **2022**, *26*, 2049−2067.

(7) Davidson, D.; Bernhard, S. A. The Structure of Meldrum's Supposed β-Lactonic Acid. *J. Am. Chem. Soc.* **1948**, *70*, 3426−3428.

(8) McNab, H. Meldrum's Acid. *Chem. Soc. Rev.* **1978**, *7*, 345−358.

(9) Chen, B. C. Meldrum's Acid in Organic Synthesis. *Heterocycles* **1991**, *32*, 529−597.

(10) Gerencsér, J.; Dormán, G.; Darvas, F. Meldrum's Acid in Multicomponent Reactions: Applications to Combinatorial and Diversity-Oriented Synthesis. *QSAR Comb. Sci.* **2006**, *25*, 439−448.

(11) Ivanov, A. S. Meldrum's Acid and Related Compounds in the Synthesis of Natural Products and Analogs. *Chem. Soc. Rev.* **2008**, *37*, 789−811.

(12) Lipson, V. V.; Gorobets, N. Y. One Hundred Years of Meldrum's Acid: Advances in the Synthesis of Pyridine and Pyrimidine Derivatives. *Mol. Diversity* **2009**, *13*, 399−419.

(13) Dumas, A. M.; Fillion, E. Meldrum's Acids and 5-Alkylidene Meldrum's Acids in Catalytic Carbon−Carbon Bond-Forming Processes. *Acc. Chem. Res.* **2010**, *43*, 440−454.

(14) Mieriņa, I.; Jure, M. Alkylidene and Arylidene Meldrum's Acids as Versatile Reagents for the Synthesis of Heterocycles. *Chem. Heterocycl. Compd.* **2016**, *52*, 7−9.

(15) Fillion, E.; Fishlock, D. Total Synthesis of (±)-Taiwaniaquinol B via a Domino Intramolecular Friedel−Crafts Acylation/Carbonyl α-Tert-Alkylation Reaction. *J. Am. Chem. Soc.* **2005**, *127*, 13144−13145.

(16) Mahulikar, P. P.; Mane, R. B. Application of Meldrum's Acid in Natural Product Synthesis. Synthesis of Ar-Turmerone and α-Curcumene. *J. Chem. Res.* **2006**, *2006*, 15−18.

(17) Fillion, E.; Dumas, A. M.; Kuropatwa, B. A.; Malhotra, N. R.; Sitler, T. C. Yb(OTf)3-Catalyzed Reactions of 5-Alkylidene Meldrum's Acids with Phenols: One-Pot Assembly of 3,4-Dihydrocoumarins, 4-Chromanones, Coumarins, and Chromones. *J. Org. Chem.* **2006**, *71*, 409−412.

(18) Da Silva, M. M. C.; de Araújo-Neto, J. B.; de Araújo, A. C. J.; Freitas, P. R.; Cícera, C. D.; Begnini, I. M.; Rebelo, R. A.; da Silva, L. E.; Mireski, S. L.; Nasato, M. C.; Krautler, M. I. L.; Ribeiro-Filho, J.; Coutinho, H. D. M.; Tintino, S. R. Potentiation of Antibiotic Activity by a Meldrum's Acid Arylamino Methylene Derivative against

Multidrug-Resistant Bacterial Strains. *Indian J. Microbiol.* **2021**, *61*, 100−103.

(19) Mehfooz, H.; Saeed, A.; Faisal, M.; Larik, F. A.; Muqadar, U.; Khatoon, S.; Channar, P. A.; Ismail, H.; Bilquees, S.; Rashid, S.; Shafique, S.; Mirza, B.; Dilshad, E.; Ahmad, F. Facile One-Pot Synthesis, Butyrylcholinesterase and α-Glucosidase Inhibitory Activities, Structure−Activity Relationship, Molecular Docking and DNA−Drug Binding Analysis of Meldrum′s Acid Derivatives. *Res. Chem. Intermed.* **2020**, *46*, 2437−2456.

(20) Mehfooz, H.; Saeed, A.; Sharma, A.; Albericio, F.; Larik, F. A.; Jabeen, F.; Channar, P. A.; Flörke, U. Dual Inhibition of AChE and BChE with the C-5 Substituted Derivative of Meldrum′s Acid: Synthesis, Structure Elucidation, and Molecular Docking Studies. *Crystals* **2017**, *7*, 211.

(21) Verma, K. N.; Mondal, D.; Bera, S. Pharmacological and Cellular Significance of Triazole-Surrogated Compounds. *Curr. Org. Chem.* **2020**, *23*, 2305−2572.

(22) Lauria, A.; Delisi, R.; Mingoia, F.; Terenzi, A.; Martorana, A.; Barone, G.; Almerico, A. M. 1,2,3-Triazole in Heterocyclic Compounds, Endowed with Biological Activity, through 1,3-Dipolar Cycloadditions. *Eur. J. Org. Chem.* **2014**, *2014*, 3289−3306.

(23) Nehra, N.; Tittal, R. K.; Ghule, V. D. 1,2,3-Triazoles of 8-Hydroxyquinoline and HBT: Synthesis and Studies (DNA Binding, Antimicrobial, Molecular Docking, ADME, and DFT). *ACS Omega* **2021**, *6*, 27089−27100.

(24) Dunn, G. L.; Hoover, J. R.; Berges, D. A.; Taggart, J. J.; Davis, L. D.; Dietz, E. M.; Jakas, D. R.; Yim, N.; Actor, P.; J V Uri, J. A. W. Orally Active 7-Phenylglycyl Cephalosporins. Structure-Activity Studies Related to Cefatrizine (SK&F 60771). *Antibiotics* **1976**, *29*, 65−80.

(25) El-Sayed, W. A.; Khalaf, H. S.; Mohamed, S. F.; Hussien, H. A.; Kutkat, O. M.; Amr, A. E. Synthesis and Antiviral Activity of 1,2,3-Triazole Glycosides Based Substituted Pyridine via Click Cycloaddition. *Russ. J. Gen. Chem.* **2017**, *87*, 2444−2453.

(26) Tian, Y.; Liu, Z.; Liu, J.; Huang, B.; Kang, D.; Zhang, H.; De Clercq, E.; Daelemans, D.; Pannecouque, C.; Lee, K.-H.; Chen, C.-H.; Zhan, P.; Liu, X. Targeting the Entrance Channel of NNIBP: Discovery of Diarylnicotinamide 1,4-Disubstituted 1,2,3-Triazoles as Novel HIV-1 NNRTIs with High Potency against Wild-Type and E138K Mutant Virus. *Eur. J. Med. Chem.* **2018**, *151*, 339−350.

(27) Angajala, K. K.; Vianala, S.; Macha, R.; Raghavender, M.; Thupurani, M. K.; Pathi, P. J. Synthesis, Anti-Inflammatory, Bactericidal Activities and Docking Studies of Novel 1,2,3-Triazoles Derived from Ibuprofen Using Click Chemistry. *SpringerPlus* **2016**, *5*, 423.

(28) El Bourakadi, K.; Mekhzoum, M. E. M.; Saby, C.; Morjani, H.; Chakchak, H.; Merghoub, N.; Qaiss, A. el kacem.; Bouhfid, R. Synthesis, Characterization and in Vitro Anticancer Activity of Thiabendazole-Derived 1,2,3-Triazole Derivatives. *New J. Chem.* **2020**, *44*, 12099−12106.

(29) Avula, S. K.; Khan, A.; Rehman, N. U.; Anwar, M. U.; Al-Abri, Z.; Wadood, A.; Riaz, M.; Csuk, R.; Al-Harrasi, A. Synthesis of 1H-1,2,3-Triazole Derivatives as New α-Glucosidase Inhibitors and Their Molecular Docking Studies. *Bioorg. Chem.* **2018**, *81*, 98−106.

(30) Avula, S. K.; Khan, A.; Halim, S. A.; Al-Abri, Z.; Anwar, M. U.; Al-Rawahi, A.; Csuk, R.; Al-Harrasi, A. Synthesis of Novel (R)-4-Fluorophenyl-1H-1,2,3-Triazoles: A New Class of α-Glucosidase Inhibitors. *Bioorg. Chem.* **2019**, *91*, No. 103182.

(31) Rehman, N. U.; Ullah, S.; Alam, T.; Halim, S. A.; Mohanta, T. A.; Khan, A.; Anwar, U. M.; Csuk, R.; Avula, S. K.; Al-Harrasi, A. Discovery of New Boswellic acid Hybrid 1*H*-1,2,3-Triazoles for Diabetic Management: In-Vitro and In-Silico Studies. *Pharmaceuticals* **2023**, *16*, 229.

(32) Fillion, E.; Fishlock, D.; Wilsily, A.; Goll, J. M. Meldrum′s Acids as Acylating Agents in the Catalytic Intramolecular Friedel−Crafts Reaction. *J. Org. Chem.* **2005**, *70*, 1316−1327.

(33) Payne, D. T.; Zhao, Y.; Fossey, J. S. Ethylenation of Aldehydes to 3-Propanal, Propanol and Propanoic Acid Derivatives. *Sci. Rep.* **2017**, *7*, No. 1720.

(34) Spivak, A. Y.; Gubaidullin, R. R.; Galimshina, Z. R.; Nedopekina, D. A.; Odinokov, V. N. Effective Synthesis of Novel C(2)-Propargyl Derivatives of Betulinic and Ursolic Acids and Their Conjugation with β-d-Glucopyranoside Azides via Click Chemistry. *Tetrahedron* **2016**, *72*, 1249−1256.

(35) Carvalho, I.; Andrade, P.; Campo, V. L.; Guedes, P. M. M.; Sesti-Costa, R.; Silva, J. S.; Schenkman, S.; Dedola, S.; Hill, L.; Rejzek, M.; Nepogodiev, S. A.; Field, R. A. 'Click Chemistry' Synthesis of a Library of 1,2,3-Triazole-Substituted Galactose Derivatives and Their Evaluation against Trypanosoma Cruzi and Its Cell Surface Trans-Sialidase. *Bioorg. Med. Chem.* **2010**, *18*, 2412−2427.

(36) Das, R.; Mukhopadhyay, B. Use of 'Click Chemistry' for the Synthesis of Carbohydrate-Porphyrin Dendrimers and Their Multivalent Approach toward Lectin Sensing. *Tetrahedron Lett.* **2016**, *57*, 1775−1781.

(37) Artyushin, O. I.; Sharova, E. V.; Vinogradova, N. M.; Genkina, G. K.; Moiseeva, A. A.; Klemenkova, Z. S.; Orshanskaya, I. R.; Shtro, A. A.; Kadyrova, R. A.; Zarubaev, V. V.; Yarovaya, O. I.; Salakhutdinov, N. F.; Brel, V. K. Synthesis of Camphecene Derivatives Using Click Chemistry Methodology and Study of Their Antiviral Activity. *Bioorg. Med. Chem. Lett.* **2017**, *27*, 2181−2184.

(38) *APEX-II*; Bruker AXS: Madison, WI.

(39) *SAINT*; Bruker AXS: Madison, WI.

(40) *SADABS*; Bruker AXS: Madison.

(41) Sheldrick, G. M. Crystal structure refinement with SHELXL-97. *Acta Crystallogr., Sect. C: Struct. Chem.* **2015**, *71*, 3−8.

(42) Alam, A.; Ali, M.; Rehman, N. U.; Ullah, S.; Halim, S. A.; Latif, A.; Zainab; Khan, A.; Ullah, O.; Ahmad, S.; Al-Harrasi, A.; Ahmad, M. Bio-Oriented Synthesis of Novel (*S*)-Flurbiprofen Clubbed Hydrazone Schiff's Bases for Diabetic Management: In Vitro and In Silico Studies. *Pharmaceuticals* **2022**, *15*, 672.

(43) Yamamoto, K.; Miyake, H.; Kusunoki, M.; Osaki, S. Crystal Structures of Isomaltase from Saccharomyces Cerevisiae and in Complex with Its Competitive Inhibitor Maltose. *FEBS J.* **2010**, *277*, 4205−4214.

(44) Molecular Operating Environment. *Chem. Comput.* Gr. ULC, 1010 Sherbooke St. West, Suite 910, Montr. QC, Canada 2020, 09.